Scholar Publishing Group
International Journal of Multimedia Computing
https://doi.org/10.38007/IJMC.2020.010104
ISSN 2789-7168 Vol. 1, Issue 1: 45-62

Visual Inspection and Batting Decision of Table Tennis Robot

Mingzhong Liu*

Hefei University of technology, Hefei, China

zjy@htc.edu.cn

**corresponding author*

Keywords: Table Tennis Robot, Visual Inspection, Batting Decision, Binocular Vision, Trajectory Tracking

Abstract: The table tennis robot is a hand-eye system that combines a visual system, a mechanical system, and a control system. The visual system is equivalent to the human brain and eyes. The visual system predicts the flight trajectory of table tennis and calculates the hitting point and hitting ball. When the time comes, the hitter can return the ball effectively. This article mainly studies the visual detection and decision-making of table tennis robots. This article introduces the method of dual target calibration, calculates the relationship between the internal parameters of the camera and the camera, and uses the calibration results to calculate the three-dimensional coordinate information of the table tennis. By comparing the existing target tracking image processing algorithms, and according to the flight characteristics of table tennis, research and formulate a set of fast real-time image processing algorithms. Through the force analysis of the table tennis in flight, the parameter model of the table tennis flight trajectory is established, and the experimental analysis of the landing point and the hitting point predicted by the flight model is carried out. In the online decision-making process, the multi-initial value quasi-Newton method is used to maximize the hitting evaluation function to solve the optimal hitting trajectory. The experimental results in this paper show that the average error of the return point of the table tennis robot in these 10 experiments is 13.4cm; the average value of the return point of the robot in 10 shots is [-2.5cm, 78.8cm], and the variance is [5.3cm, 13.4cm]; The average value of the person's return point is [-3.1cm, 13.9cm], and the variance is [11.6cm, 22.9cm]. The experimental results of this paper show that the return accuracy of table tennis robots is better than those who have little experience in hitting the ball; table tennis robots can adapt to changes in the state of the incoming ball and complete the fixed-point return task with higher accuracy and success rate.

1. Introduction

1.1. Background and Significance

The key technologies of robots include target recognition and tracking, path planning, multi-sensor information fusion and other related technologies. They are widely used in application scenarios such as hotel service robots, autonomous driving, drones and missile interception. Among them, the identification and tracking of fast flying objects are of great research and application value in the identification and tracking of suspicious targets in sports competition monitoring and adjudication and military confrontation. Because most objects are very fast when flying, and sometimes have rotation, or even high-speed rotation, the rapid identification and tracking of high-speed rotating objects is extremely challenging.

Machine vision extracts target information from the objective environment and achieves the goal of target detection and control through image processing and understanding [1]. “Real-time” is the most important technical requirement of table tennis robot vision system. This is also a different aspect of table tennis robot vision technology from traditional image processing. The system involves many cutting-edge issues such as visual recognition, intelligent control, deep learning, etc., and has a huge role in promoting the development of intelligent robots [2-3]. Therefore, in this paper, in-depth study of the table tennis robot's visual detection and ball hitting decision methods for the above problems.

1.2. Development Status of Table Tennis Robots at Home and Abroad

In 1983, the United Kingdom designed a table tennis robot that can play against. Although the robot can play against people, there are many restrictions on this robot, and it is very different from the regulations of international table tennis competitions. The size of the table is 2m*0.5m [4-5]. The stipulated size is very different from the size of the international standard table tennis table, the width is equivalent to one third of the international standard, and the length is 74cm smaller than the international standard [6-7]. And the table tennis that the person hits must pass through the three detected metal frames at the same time in order to detect the flight path of the ball, and when the person returns to the ball, the racket can only move and intercept in front of the metal frame in front of himself [8-9].

In 2002, a table tennis robot appeared, capable of hitting the ball with rotation. The robot has a binocular stereo vision system [10-11]. This robot is developed by Japan, it has four degrees of freedom, mainly composed of two rotating mechanisms and two translation mechanisms, which is different from other robots in that it can hit the table tennis to a specified position, And can return to the ball with many changes, that is, with a rotating ball [12-13]. But at the same time, it is necessary to install relevant sensors on the human arm to detect the rotation direction of the ball, and the robot has a strong ability to return the ball [14-15].

In China, the research on table tennis robots is relatively late. The first generation of table tennis robot, which has a monocular vision system, and is a double racket, with a rotating robotic arm, due to the monocular vision system, only two-dimensional information, you need to use other auxiliary information to calculate the three-dimensional table tennis information [16-17]. Therefore, the first generation of table tennis robots used ball shadows to calculate three-dimensional information. For the three-dimensional information obtained by this method, the algorithm is complicated. Although the CPU of P4.30GHZ was used at that time, the obtained three-dimensional coordinates also had a time delay. Problem, and the robot's batting success rate is low, around 60% [18]. In response to this

problem, Zhejiang University of Technology has deepened the analysis of table tennis robots. The mechanical structure of the robot is based on Japanese table tennis robots and has been improved. The driving mechanism of the mobile mechanism is driven by pulleys. The monocular vision system is changed to a binocular vision system, and the algorithm is modified to use "sliding window filtering method based on least squares method" and "Kalmam filtering method based on adaptive covariance". It is also structurally and visually there are a lot of optimization changes in the algorithm, so the trajectory tracking of the table tennis has been greatly optimized. It can play multiple rounds with people at the same time.

The original table tennis robot's visual system was to install four cameras on the table tennis table. The total field of view of the four cameras covered the entire table tennis table, and the common area of the field of view between the cameras was only half of the table. Therefore, the range of table tennis is very limited [19]. The system involves multiple cameras, the introduction of cameras to calculate the coordinate size must be calibrated, and multiple cameras involve the problem of calibration between multiple cameras, and the common field of view between cameras is less, which makes the pose between the cameras The relationship can only be guaranteed by the precision of the processed parts, so the accuracy of the calculated three-dimensional coordinates cannot be guaranteed [20-21].

Someone has developed a table tennis robot that uses only one camera's vision system. For a monocular system, it can only obtain two-dimensional information, but not three-dimensional information, so another three-dimensional calculation method has been proposed. In addition to using a camera, the vision system also uses an auxiliary light source. The purpose of the light source is to let the table tennis illuminate the ball shadow on the desktop. The vision system uses the information of the ball shadow and the image information of the table tennis to calculate the three-dimensional coordinates [22-23]. The above vision systems are the three types of vision systems used since the development of table tennis robots. Although the vision system was used to track and predict the movement of table tennis at that time, in the vision system at that time, the development of PC hardware Behind, the image processing speed cannot keep up, so that the calculated table tennis coordinates and the accuracy of the predicted table tennis trajectory cannot be guaranteed well [24-25]. According to Japanese video recordings of table tennis robots, the robot simply cannot react when the ball speed is relatively fast, so the visual system at that time was not suitable for detecting high-speed moving objects [26-27].

1.3. Related Work

Padulo J studied the impact of intensive exercises on perception, decision-making and motor systems in table tennis. He passed the reaction time test and reaction time test on all subjects, including pointing the target at different distances (15 and 25 cm) to the right and left. Only the HL and LL groups are required to perform the ball speed test in the forehand and backhand states. His experimental results found that the reaction time of the CC group was longer than that of the HL group ($P < 0.05$). He concluded that the response time of table tennis players is shorter than that of non-athletes, and the task of reaction time and response time cannot distinguish the performance of well-trained table tennis players and intermediate players, but the ball speed test seems to be able to do it [28]. *Zhang* proposed a vision-based table tennis robot to estimate the opponent's hitting point, which can better understand the opponent, thereby improving the reaction speed of the table tennis robot. As an important manifestation of the opponent's hitting behavior, the hitting point information includes not only the movement state of the ball before and after hitting but also the

racket posture at the moment of hitting. Considering that the trajectory of the ball and racket are not absolutely accurate, he proposes an optimized solution to calculate the opponent's hitting point. The method he proposed is the first method that can quickly estimate the opponent's hit point with a satisfactory resolution [29]. *Su* developed a model to calculate the expected return ball speed so that the robot can return the input ball to the desired point on the table at the specified landing speed. He designed fuzzy rules by analyzing the effect of expected speed on the error between the actual landing point and the expected point. According to the landing point error predicted by the flight model, he uses a fuzzy correction algorithm to obtain the final return speed of the ball. Finally, he verified the effectiveness of the proposed method through experiments [30].

1.4. Innovation in this Article

The main innovations of this paper include the following aspects: (1) this paper proposes a concise and easy-to-implement method for solving the range of arm angles, and proves the existence of the reference plane to ensure that the inverse kinematics algorithm can achieve Feasibility; and proved the effectiveness of the algorithm through theoretical derivation and experimental verification. (2) Aiming at the motion blur introduced by high-speed sports table tennis in visual measurement, a table tennis position measurement method based on motion blur parameter identification is proposed. This method first estimates the blur kernel parameters based on the directional filter, and then deconvolves the image to obtain the deblurred image, and finally performs a circle fitting to obtain the position of the table tennis ball in three-dimensional space. The method in this paper can effectively reduce the effect of motion blur on binocular visual positioning and improve the accuracy of table tennis three-dimensional position measurement.

2. Table Tennis Trajectory Prediction Algorithm

2.1. Image Segmentation Based on Background Subtraction

(1) Area segmentation algorithm selection

After learning and experimenting with color recognition and frame difference method, we found that the background in the real environment is fixed, and only table tennis is in motion. Therefore, background subtraction may be the best choice. The background subtraction method is to compare the current frame with the background frame, and then subtract the known background frame information. The remaining information is the target foreground information and the initial result of the target area segmentation.

The establishment of the background model is the key to the background subtraction algorithm. "Background" is a difficult concept to define. On different occasions, the background is different. In general, the background can be defined as a target that presents a static state or a periodic motion state in the scene during any period of interest. Through a deep understanding of the experimental environment, the scene information without target information is used as background information. We can see the foreground information clearly and completely. Therefore, the background subtraction method is used as the target region segmentation algorithm. In addition, it can also be seen that the target information obtained by using the background subtraction method contains a large amount of noise, which requires subsequent processing.

2.2. Morphological Operation of Binary Image

This article uses morphological operations to achieve the purpose of eliminating noise. Mathematical morphology is a technology and science for analyzing and processing geometric structures based on topology, lattice theory, set theory, and stochastic processes. Mathematical morphology is often used in digital images, but it can also be used in graphics, grids and other spatial structures. Mathematical morphology is the foundation of morphology. Morphological operation is a neighborhood operation. The morphological operation process is a specific logical operation between each pixel in the image and its corresponding neighborhood. This specially defined neighborhood is called "structural element". The effect of morphological operations depends on the shape, size and logical operations of structural elements. The common element shapes are round, square and diamond. The specific structure is shown in Figure 1.

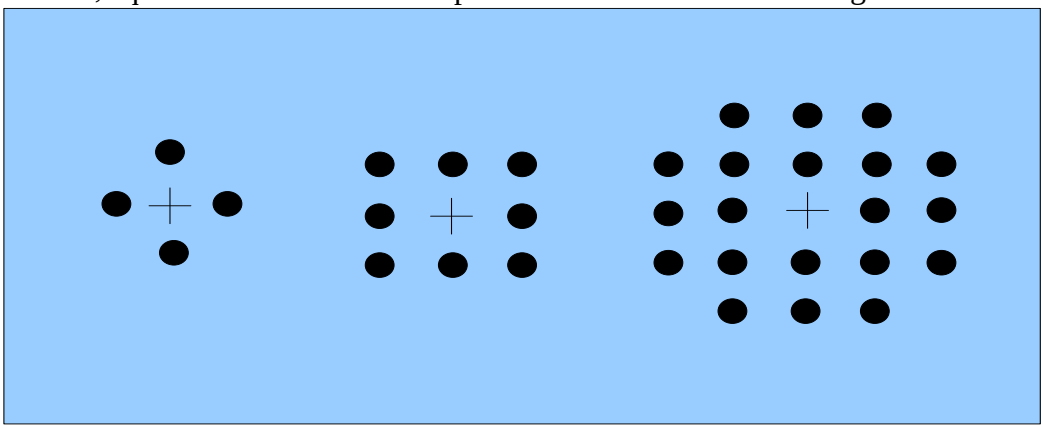

Figure 1. Common structural element shapes

2.3. Edge Detection

The edge detection network is an end-to-end detection system. The VGG16 network structure performs well on ImageNet. It contains 16 convolutional layers and has a great depth. Most of the previous saliency detections used only one network branch, which was only set up to achieve a task, but after research It is found that there is a certain relationship between the saliency detection of images, edge detection and contour detection of salient objects. If this connection can be discovered and used to establish a relationship between the two networks, this connection can be used to help the saliency detection model improve performance. Based on this starting point, through a lot of experiments, it has been found that the feature map output by the edge detection network can help the saliency detection model to better detect the boundary between the foreground target and the background to a certain extent. For the saliency detection of images with low background contrast, it is very helpful. Therefore, this paper proposes a network model based on edge detection for saliency detection.

This paper uses the results of edge detection to improve the performance of the saliency detection model. The algorithm framework is divided into two parts, namely the edge detection part and the saliency detection part. Among them, the edge detection part uses the VGG16 network structure to perform edge detection on the image, and the saliency detection part uses the UNet network structure to achieve salient object detection. First, the edge detection branch network is trained. The BSDS500 database is used for network training. After the edge detection branch network training is completed, the parameters are saved to participate in the next stage of saliency

detection training. In the saliency detection branch network, the short connection layer of the UNet network structure makes the features of the image in the downsampling stage fully utilized in the upsampling stage, that is, the fusion of the underlying features, on this basis, the edge

Detect the feature map output in each convolutional layer in the branch structure, and each layer in the deconvolution stage is separately fused by the edge fusion module, where the deconvolution module is a custom deconvolution on the UNet network structure. The green branch in the upper half is the edge detection network structure, which uses the VGG16 network framework. Unlike the original network, we have made two changes, that is, removing the fully connected layer and the fifth pooling layer, and in each A side output layer is added to the last convolutional layer of a convolution stage. From Conv1 to Conv5 are the five convolution stages, from 1 map to 5 map are the feature maps output by the last convolutional layer through the side output layer of each convolution stage, and each output feature map uses edges Truth value to monitor, and finally return the total loss to the network. Finally, the five feature maps are cascaded through the green C module, and then fused through the F module to form the final edge map output. The orange and red branches in the lower part of the figure are the convolution operation and the deconvolution operation part of the UNet network structure. The convolution part uses the UNet network's own convolution layer, and the deconvolution part is customized by this article. A deconvolution layer, the detailed structure will be explained later. The EF module is an edge fusion module that fuses the feature map output from the output layer of the edge detection network and the feature map output from each deconvolution layer of the saliency branch network, and combines the feature map after edge fusion with the convolution stage The output feature map is fused through the gray C module, and then the next deconvolution operation is performed. The saliency map output by each deconvolution layer is supervised by a truth map, and the calculated losses are summed back to the network, and the next training is continued.

The deep neural network pre-trained on the general classification task is very effective for the task of low-level edge detection, so the structure of this edge detection network is VGG16. Compared with the original VGG16 structure, the edge detection network structure in this paper has two changes: One is that a side output layer is added to the last layer of each convolution stage, that is, Conv1_2, Conv2_2, Conv3_3, Conv4_3, Conv5_3 Behind. The second is to remove the fifth pooling layer and the fully connected layer of the network. This is because the size of the output image of the last convolutional layer is 1/32 of the original image. If interpolation is performed, the resulting prediction image will be too vague to be used. In addition, the calculation of the fully connected layer is too large, which will increase the memory and time costs of the training and testing phases. Therefore, after transformation, the convolution part is divided into five convolution operation stages. First, the image is adjusted to a size of 384×384. After the convolution layer is used for feature extraction, the final feature map size is 12×12. 1/32 of the size. During the convolution operation, the underlying features of the image edges, details, etc. are mostly distributed in the first few convolutional layers, so this paper extracts the feature map output by the last convolutional layer of each stage as the side output. A convolutional layer with a convolution kernel of 1×1 changes the number of feature map output channels to 1, where the second to fifth side outputs have to undergo upsampling operations so that the size is the same as the first side output, and then used separately The edge truth map is supervised, and then these feature maps are connected, and finally sent to the fusion structure for feature fusion, so that the resulting fusion map will have different scales of feature information from each layer. The edge truth map has been supervised, so most of the information is the edge part of the image, which is of great help to the final output edge map.

3. Table Tennis Flight Trajectory Modeling

(1) Analysis of force in table tennis flight

The force analysis of table tennis in flight is shown in Figure 2. During the flight, it is mainly affected by gravity and air resistance. If the table tennis rotates during flight, the Magnus force will be introduced. The force formula of table tennis in flight is as follows:

$$F_G = -mg \tag{1}$$

$$F_S = \rho\omega T_b S C_L V \tag{2}$$

$$F_b = \frac{1}{6}\pi\rho d^3 g \tag{3}$$

$$F_m = \frac{1}{2}\rho\omega T_b S C_L V \tag{4}$$

Where g is the acceleration of gravity, m is the mass of the table tennis ball, ω is the rotation angular velocity of the table tennis ball, ρ is the air density, r_b ball radius, and d is the ball diameter. V The speed of the ball, s is the effective area of the ball, C_D is the air resistance coefficient, and C_L is the ascent coefficient.

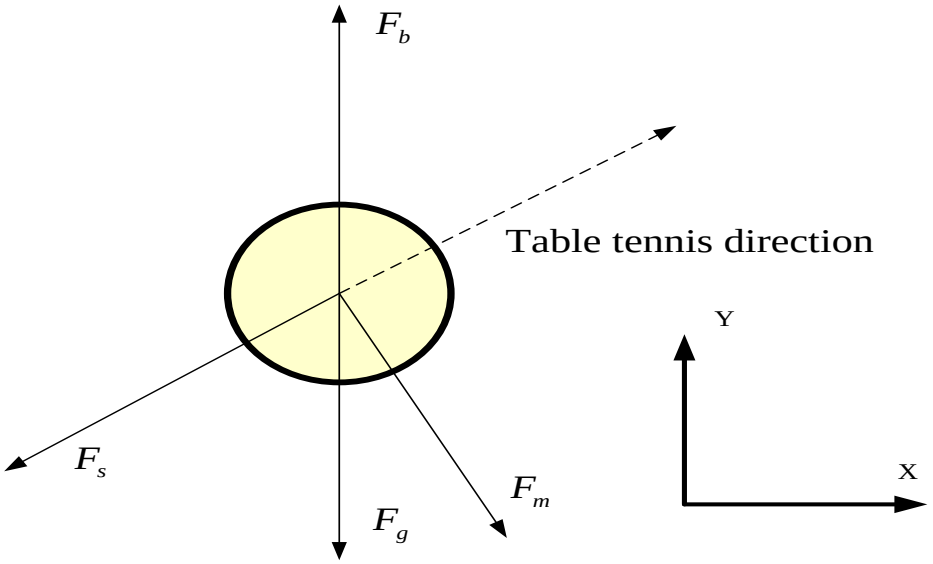

Figure 2. Schematic diagram of force analysis during table tennis flight

The magnitude of buoyancy is shown by formula (5):

$$F_b = \frac{4}{3}\rho g\pi r^3 = \frac{1}{6}\pi\rho d^3 g = \frac{1}{6}\times 3.1416\times 1.169\times 0.040^3\times 9.8 = 3.8\times 10^{-4} N \tag{5}$$

If the table tennis flight speed is too fast, the robot will fail to hit the ball. Therefore, it is assumed that the table tennis flight speed is 3m / s, the angular speed is 5rad / s, and the range of

ddddddddddd is 0.4-0.5. From equation (6), the rotation force of the table tennis is calculated to be 0.1017×10^{-2}N. The gravity of table tennis is 2.0×10^{-2}N as shown by equation (7). The air resistance is calculated by formula (8) in the range of $0.2916 \times 10^{-2} \sim 4.0506 * 10^{-2}$N. The calculated buoyancy of the table tennis in flight is as much as two orders of magnitude higher than the air resistance and gravity, so the table tennis buoyancy in flight is negligible.

$$\left\| \vec{F}_M \right\| = \rho \omega T_b S C_L \left\| \vec{v}_M \right\| = 0.1017 \times 10^{-2} N \tag{6}$$

$$\left\| \vec{F}_G \right\| = mg = 2.0 \times 10^{-2} N \tag{7}$$

$$\left\| \vec{F}_D \right\| = \frac{1}{2} \rho S C_D \left\| \vec{V} \right\| = 0.2916 \times 10^{-2} \sim 4.0506 \times 10^{-2} N \tag{8}$$

Excluding the above-mentioned various factors, the analysis of the force of table tennis during the flight can be considered as: only affected by gravity and air resistance, thus formula (9) is obtained.

$$\left\| \vec{F}_D \right\| = \frac{1}{2} \rho S C_D \left\| \vec{V} \right\| = 0.2916 \times 10^{-2} \sim 4.0506 \times 10^{-2} N \tag{9}$$

Among them:

$$\vec{F}_D = \frac{1}{2} \rho S C_D \left\| \vec{V} \right\| \vec{V} \tag{10}$$

$$\vec{F}_G = \begin{bmatrix} 0 & -mg \end{bmatrix}^T \tag{11}$$

(2) Table tennis flight trajectory model

Differentiating formula (9) gives the following formula (12):

$$\begin{bmatrix} x \\ y \\ z \\ V_x \\ V_y \\ V_z \end{bmatrix} = \begin{bmatrix} V_x \\ V_y \\ V_y \\ -K_m V_x^2 \\ -K_m V_y^2 \\ -K_m V_z^2 \end{bmatrix} \tag{12}$$

$$K_m = \frac{1}{2m} \rho S C_D \tag{13}$$

According to the parameter value range involved in formula (13), it can be known that the value range of K_m is between 0.10-0.2.

By discretely separating formula (12), the following formula (14) can be obtained:

$$\begin{bmatrix} x_i \\ y_i \\ z_i \\ V_{xi} \\ V_{yi} \\ V_{zi} \end{bmatrix} = \begin{bmatrix} x_{i-1} \\ y_{i-1} \\ z_{i-1} \\ V_{xi-1} \\ V_{yi-1} \\ V_{zi-1} \end{bmatrix} + \begin{bmatrix} V_{xi} - 1 \\ V_{yi} - 1 \\ V_{zi} - 1 \\ -K_m \left\| \overline{\omega}_{xi-1} \right\| v_{xj-1} \\ -K_m \left\| \overline{\omega}_{yi-1} \right\| v_{yj-1} \\ -K_m \left\| \overline{\omega}_{zi-1} \right\| v_{zj-1} \end{bmatrix} \tag{14}$$

Where T_c is the iteration step size, i = 1,2,3,4,5 ... n, as can be seen from the above formula, as long as you know the three-dimensional coordinates of the table tennis ball at a certain moment and the X, Y, Z directions Speed, you can solve the parabolic equation of table tennis flight trajectory by least square method.

4. Experimental Simulation Design of Table Tennis Robot

4.1. Table Tennis Robot Experimental Platform

Table tennis robot system can be divided into three subsystems: binocular vision system, control decision system and execution system. The overall architecture of the system is shown in Figure 3, including: a binocular image acquisition system based on a high-speed CCD camera and a PC-based image processing system, a control decision system based on an embedded real-time operating system, and a seven-degree-of-freedom humanoid arm Execution system.

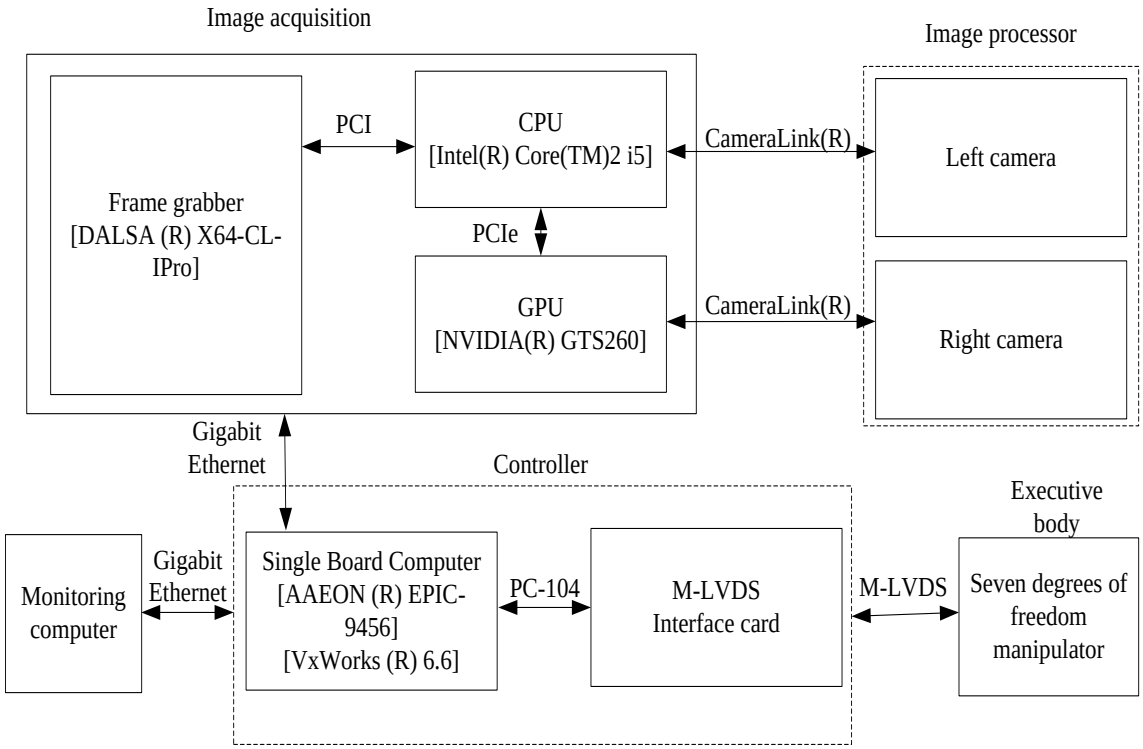

Figure 3. Table tennis robot system architecture

4.2. Experimental Design of Batting Decision

Figure 4. Machine perspective detection diagram

As shown in Figure 4, it is the effect of edge detection in this paper.As shown in Figure 5, a schematic diagram of the ping pong robot studied in this paper. This paper uses a fixed-point return experiment to initially verify the method of hitting decision-making based on support vector regression. In the fixed-point return experiment, the table tennis serve machine is used as the opponent of the table tennis robot. The expected return position is set to [0,70cm, 2cm], and R is set to 40.0cm. During the test, the incoming ball speed varied from 370cm / s to 520cm / s to test the adaptability of the hitting strategy to different incoming ball trajectories. In the batting test, the return rate of the ball-bearing robot is 92%. The expected hitting point for this shot planning is [-17.6cm, -134.3cm, 21.1cm], the hitting speed is 119.0cm / s, the pitch angle and deflection angle of the hitting trajectory are -25.2 °and- 1.0 °. The points on the trajectory are obtained from the joint angles collected in real time through the positive kinematics of the robot arm.

Figure 5. Table tennis robot

Because the robot arm requires greater acceleration in the preparation and end phases, the tracking error is larger, but the tracking error in the preparation and end phases has no effect on the shot. In the hitting stage, the tracking error of each joint of the robot arm is less than + 0.5 °, which can meet the requirements of accurate hitting planning.

Table 1. State statistics

ID	State of arrival		
	$[x_{vp}, z_{vp}](cm)$	$\upsilon_{vp}(cm/s)$	$x_m(cm)$
1	[-13.0,46.8]	[-15.0,-430.0,-42.0]	[-17.6,-134.3,21.1]
2	[-10.8,35.1]	[-34.8,-508.5,-107.1]	[-21.0,-128.2,18.0]
3	[-10.0,29.5]	[-39.2,-508.9,-64.9]	[-17.4,-122.0,14.2]
4	[-9.9,34.3]	[-32.2,-503.2,-125.9]	[-13.8,-127.4,16.9]
5	[-28.7,38.0]	[23.2,-434.3,-84.8]	[-23.0,-131.7,21.3]
6	[-19.7,42.3]	[26.5,-371.4,-41.9]	[-11.9,-131.0,20.9]
7	[-19.0,31.6]	[15.2,-421.4,-127.0]	[-18.1,-124.1,11.7]
8	[-9.1,37.7]	[-26.6,-520.7,-100.9]	[-17.9,-124.6,21.0]
9	[-9.6,34.1]	[-30.8,-494.3,-111.5]	[-20.1,-122.6,16.0]
10	[-10.8,33.0]	[-32.8,-492.2,-124.8]	[-18.9,-128.2,13.9]

As shown in Table 1 and Table 2, the ball arrival status, ball trajectory and ball return point error during the 10 consecutive ball strikes. In these 10 experiments, the average error of the return point of the table tennis robot is 13.4cm. It can be seen from the experiment that the table tennis robot can adapt to the change of the incoming ball state and complete the fixed-point return task with higher accuracy and success rate.

Table 2. Ballistic trajectory parameters and landing point error statistics

ID	Ball trajectory parameters				Falling point error(cm)
1	$t_m(s)$	$v(cm/s)$	$\alpha(°)$	$\gamma(°)$	
2	0.54	119.0	-1.0	-25.2	14.8
3	0.52	96.7	-0.6	-26.2	18.8
4	0.44	107.1	-1.0	-26.4	19.2
5	0.57	90.9	-0.6	-28.0	22.8
6	0.53	110.3	1.1	-25.7	2.0
7	0.63	152.0	0.5	-30.0	8.4
8	0.58	121.8	-1.2	-26.9	3.2
9	0.51	93.7	-1.5	-27.5	2.8
10	0.52	103.5	0	-25.2	15.2

5. Play against People

5.1. Analysis of the Fight against People

In the playing experiment, the ping pong robot collaborates continuously with people to hit the ball. Playing with people requires table tennis robots to adapt to different incoming ball trajectories and make corresponding batting decisions. Therefore, high requirements are placed on the effectiveness of the robot's batting strategy and the real-time and reliability of robot systems. After training, the table tennis robot can complete multiple rounds of continuous shots with humans, as shown in Figure 6, which is a histogram of the number of robot shots during the test. The robot can complete 8 consecutive rounds of hitting with a human. The average number of hits of the robot

during the entire test is 4.26 ±1.98.

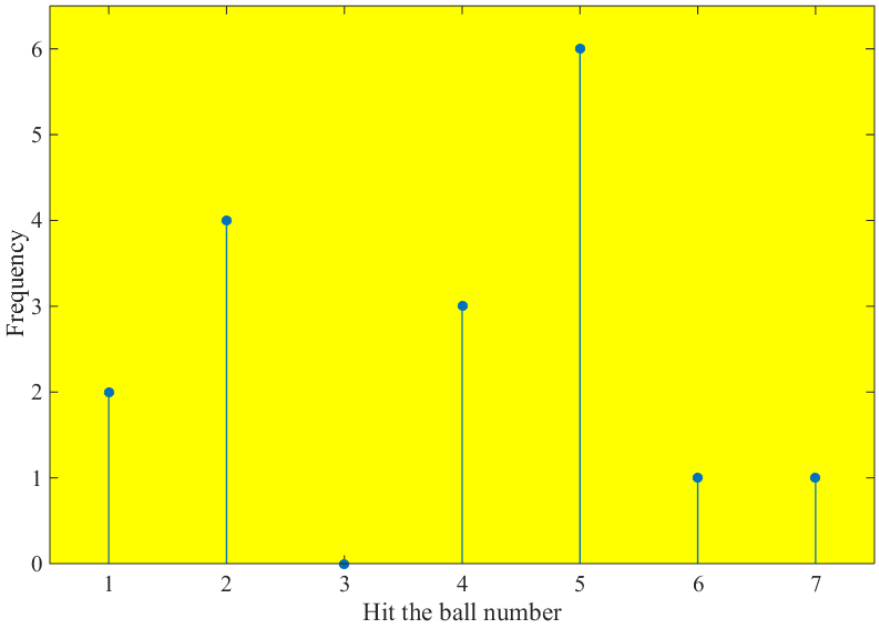

Figure 6. Table tennis robot hits

The batting process included a total of 6 rounds. Finally, the ping-pong robot incorrectly selected a large batting speed to cause the ball to go out of bounds and ended. According to the system log, in the first round, the table tennis robot completed the return task with a higher accuracy, and the distance from the drop point to the expected drop point was 13cm; in the second round, the table tennis robot chose a larger hitting speed, Therefore, the return point of the table tennis ball is close to the edge of the table, and the error of the landing point is 41cm; during the third shot, the trajectory of the ball is biased to the right of the table tennis robot by about 16cm compared with the previous two. The hitting point was correctly selected, but the hitting direction was not towards the center of the table, causing the return point to deviate to the right by about 20cm; during the fourth hit, the table tennis robot with the trajectory deviating to the right was correctly selected The hitting point, direction and speed are successful, and the ball is returned to the center line of the table. It can be seen from this that in the process of hitting the ball, the table tennis robot tries to return the ball to the desired landing point based on the learned hitting strategy, that is, to complete the fixed-point return task.

5.2. Contrast Analysis of Ball Return Accuracy

As shown in Figure 7, the average value of the robot's falling point in ten shots is [-2.5cm, 78.8cm], and the variance is [5.3cm, 13.4cm]; the average value of the person's returning point is [-3.1cm, 13.9cm], the variance is [11.6cm, 22.9cm]. That is, the return accuracy of the table tennis robot is better than those who have little experience in hitting the ball.

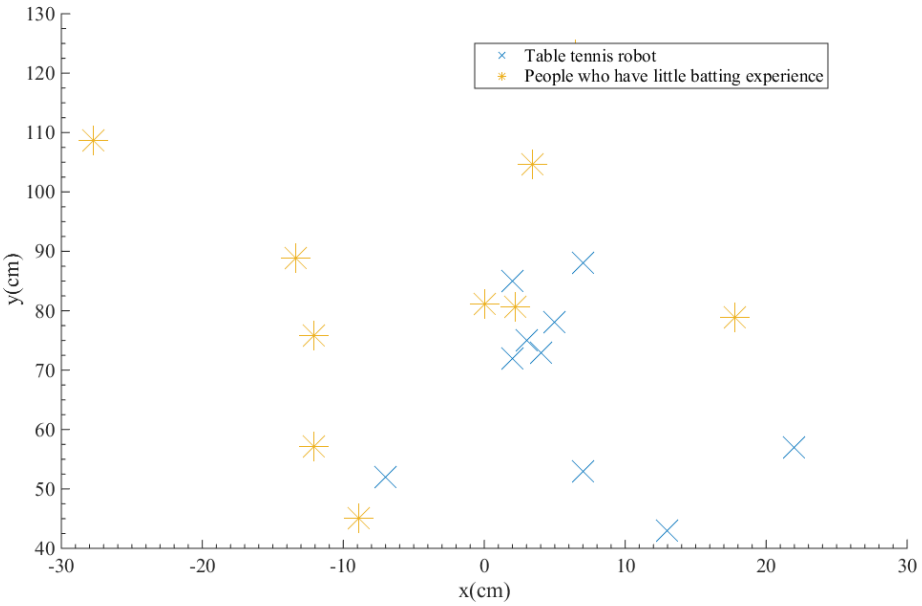

Figure 7. Table tennis robot's return point

5.3. Recognition of Batting Action

As shown in Table 3 and Table 4, using the maximum value of the signal, the minimum value of the signal and the average of the signal characteristics in the three directions of x, y, z, a total of 9-dimensional features are used to predict the action and then make the final Compared with the traditional DTW algorithm, dynamic time warping matching has a significant improvement in algorithm efficiency under the condition of little effect on the action recognition rate.

Table 3. DTW recognition rate and time statistics

Classification	DTW recognition rate	Time cost	Improved DTW recognition rate	Time cost
Right hand attack	80%	0.183s	81%	0.164s
Right hand rub	83%	0.212s	81%	0.177s
Left hand attack	78%	0.188s	78%	0.166s
Left hand rub	82%	0.202s	81%	0.181s
Left hand push	89%	0.161s	89%	0.149s

Table 4. Recognition rate and time statistics of other algorithms

Classification	K-NN recognition rate	Time cost	Decision tree recognition rate	Time cost
Right hand attack	64%	0.235	71%	0.202
Right hand rub	66%	0.277	67%	0.161
Left hand attack	66%	0.313	65%	0.142
Left hand rub	71%	0.271	64%	0.191
Left hand push	77%	0.213	75%	0.105

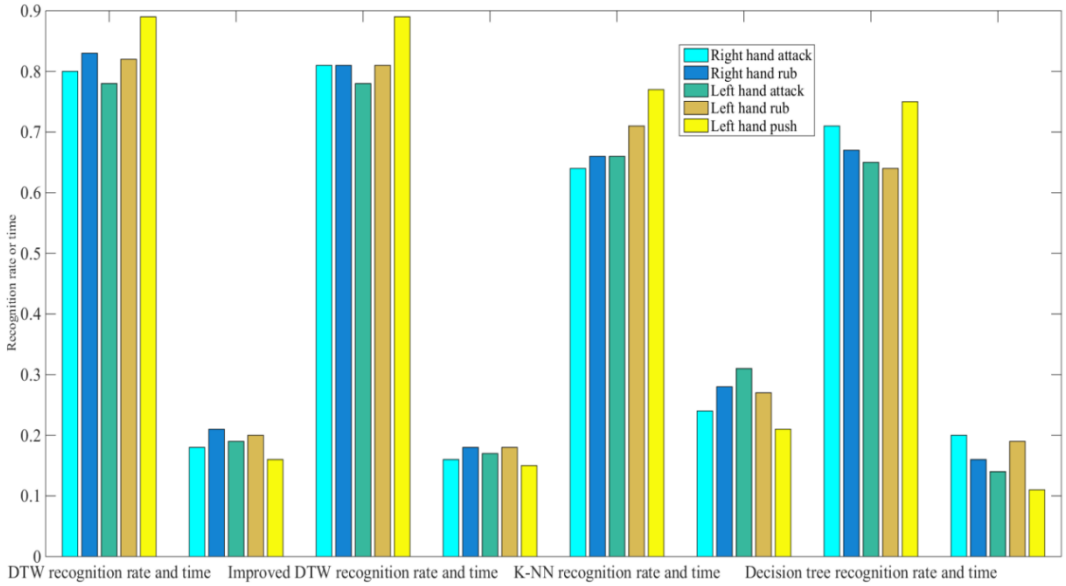

Figure 8. Comparison of action classification results

As shown in Figure 8, in order to further illustrate that the improved DTW algorithm has better recognition rate and accuracy than other algorithms, the k-NN algorithm and the decision tree algorithm are used in the experiment to classify these five sets of actions. Recognition, it can be found that the DTW recognition algorithm recognizes five types of table tennis batting action recognition rate are higher than k-NN algorithm, and decision tree recognition algorithm [31-35].

5.4. Analysis and Comparison of Classification and Recognition Algorithms

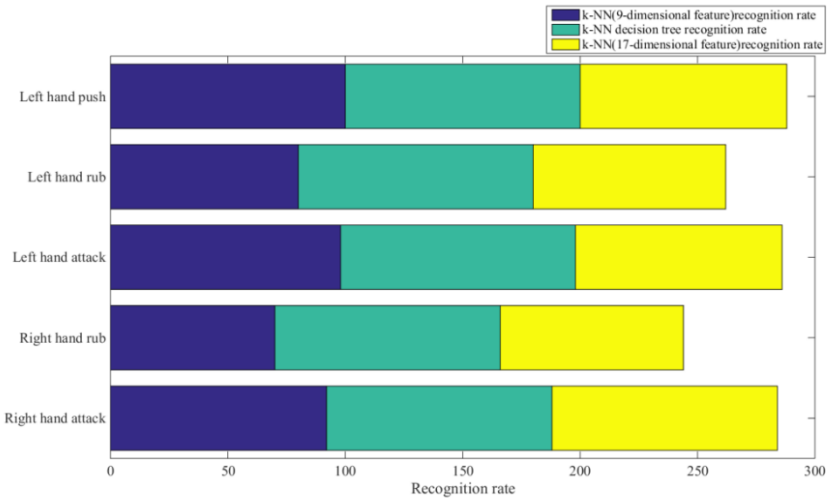

Figure 9. Analysis and comparison of classification and recognition algorithms

As shown in Figure 9, compared to other algorithms, the K-NN algorithm is simple and easy to implement. When each action in the sample library has enough training samples, high recognition

accuracy can be obtained. However, it is easy to cause the failure to filter the features. The generation of redundant features affects the efficiency of the algorithm. The improved decision tree algorithm has a clear hierarchical category structure, and the calculation amount is smaller than other algorithms. But the algorithm is prone to misjudgment for noisy action signals, which is also the biggest disadvantage of traditional decision tree algorithm. The improved dynamic time warping algorithm can achieve more accurate matching compared to other algorithms when processing motion signals with time axis displacement, so the recognition rate is higher than other algorithms. The process of DTW algorithm for similarity matching is more complicated than other algorithms, so the algorithm is inefficient and the identification takes a long time.

6. Conclusion

This paper analyzes the characteristics of table tennis robots, formulates a set of high-speed target contour extraction methods according to the table tennis flight characteristics, and analyzes the contour characteristics according to the characteristics of table tennis flight to extract target contours better and faster. Create a table tennis flight trajectory model and optimize it. The table tennis flight trajectory is divided into three stages for analysis and optimization. And according to the location of the table tennis table, strategically solve the hitting point.

Aiming at the problem of table tennis robot's batting decision, this paper proposes a batting decision algorithm based on support vector regression. The table tennis robot's batting process is formalized as a batting evaluation function. Then, based on the training data set and the support vector regression algorithm, an approximate estimate of the batting evaluation function is obtained. Finally, for a specific incoming ball, the optimal impact evaluation function can be obtained by optimizing the impact evaluation function with the impact trajectory parameters as variables. The fast evaluation and optimization of the batting decision function are realized, thereby reducing the time required for batting decision.

This paper realizes the rapid recognition and tracking of target objects. First, the color-based image segmentation algorithm, the difference method and the background subtraction method are compared, and it is found that the background subtraction method performs best as a subdivision algorithm for the target area. Then the opening and closing operations and edge detection operations are performed on the target area for the first division. Then the random Hough circle transformation is used to identify the target object, and the position in the target is obtained. Finally, a local area search algorithm based on the previous detection target is proposed, which realizes the real-time detection and tracking of the three-dimensional position space of table tennis at high speed.

Funding

This article is not supported by any foundation.

Data Availability

Data sharing is not applicable to this article as no new data were created or analysed in this study.

Conflict of Interest

The author states that this article has no conflict of interest.

References

[1] Michael Fuchs, Ruizhi Liu, Ivan Malagoli Lanzoni. Table Tennis Match Analysis: A Review. J Sports Sci, 2018, 36(3):1-10. https://doi.org/10.1080/02640414.2018.1450073

[2] Fengqin Fu, Yan Zhang, Shirui Shao. Comparison of center of pressure trajectory characteristics in table tennis during topspin forehand loop between superior and intermediate players. Japanese Journal of Clinical Oncology, 2016, 11(4):126-131. https://doi.org/10.1177/1747954116654778

[3] Tamer Karademir, Ünal Türkçapar. Examination of Anxiety Levels and Anger Expression Manners of Undergraduate Table Tennis Players. Universal Journal of Educational Research, 2016, 4(10):2274-2281. https://doi.org/10.13189/ujer.2016.041005

[4] Zhou J D, Yuan F, Yu T, et al. Why are the disabled people willing to participate in sports: taking Chinese disabled table tennis players as the object of investigation?. Advances in Physical Education, 2016, 06(2):88-98. https://doi.org/10.4236/ape.2016.62010

[5] Yann Le Mansec, Sylvain Dorel, François Hug. Lower limb muscle activity during table tennis strokes. Sports Biomechanics, 2017, 17(4):1-11. https://doi.org/10.1080/14763141.2017.1354064

[6] Ziemowit Bankosz, Slawomir Winiarski. The kinematics of table tennis racquet. The differences between topspin strokes. Journal of Sports Medicine & Physical Fitness, 2017, 57(3):202-213. https://doi.org/10.23736/S0022-4707.16.06104-1

[7] Byung-chun You, Won-Jae Lee, Seung-Hwa Lee. Shoulder Disease Patterns of the Wheelchair Athletes of Table-Tennis and Archery: A Pilot Study. Annals of Rehabilitation Medicine, 2016, 40(4):702. https://doi.org/10.5535/arm.2016.40.4.702

[8] Qi Zhao, Yingzhi Lu, Kyle J. Jaquess. Utilization of cues in action anticipation in table tennis players. Journal of Sports Sciences, 2018, 36(23):1-7. https://doi.org/10.1080/02640414.2018.1462545

[9] Haeok Lee, Younhee Kang, Woong Ju. Cervical Cancer Screening in Developing Countries: Using Visual Inspection Methods. Clinical Journal of Oncology Nursing, 2016, 20(1):79-83. https://doi.org/10.1188/16.CJON.79-83

[10] Sho Uehara, Hajime Kawahara, Kento Masuda. Transiting Planet Candidates Beyond the Snow Line Detected by Visual Inspection of 7557 Kepler Objects of Interest. Astrophysical Journal, 2016, 822(1):2. https://doi.org/10.3847/0004-637X/822/1/2

[11] Mustafa, RA, Santesso, N, Khatib, R. Systematic reviews and meta-analyses of the accuracy of HPV tests, visual inspection with acetic acid, cytology, and colposcopy. International Journal of Gynaecology & Obstetrics the Official Organ of the International Federation of Gynaecology & Obstetrics, 2016, 132(3):259-265. https://doi.org/10.1016/j.ijgo.2015.07.024

[12] Misra A, Vaibhaw K, Singh R, et al. A Study of Cervical Cancer Screening by Acetic Acid in Visual Inspection in District Hapur U.P. India. Indian Journal of Public Health Research & Development, 2016, 7(4):18. https://doi.org/10.5958/0976-5506.2016.00181.9

[13] Gabriel Olusegun Emmanuel, Dada Ayokunle. Reliability of Visual Inspection After Acetic Acid Staining in Screening for Cervical Pre-malignant Lesion Among Female Subjects in a Rural Tertiary Hospital in Nigeria. Naunyn Schmiedebergs Archiv Für Experimentelle Pathologie Und Pharmakologie, 2016, 4(1):1. https://doi.org/10.11648/j.crj.20160401.11

[14] Martyushenko N, Almaas E. ModelExplorer - software for visual inspection and inconsistency correction of genome-scale metabolic reconstructions. BMC bioinformatics, 2019, 20(1):56. https://doi.org/10.1186/s12859-019-2615-x

[15] Asgary, Ramin, Adongo, Philip Baba, Nwameme, Adanna. MHealth to Train Community Health Nurses in Visual Inspection with Acetic Acid for Cervical Cancer Screening in Ghana. Journal of Lower Genital Tract Disease, 2016, 20(3):239. https://doi.org/10.1097/LGT.0000000000000207

[16] Orang'O O, Elkanah, Liu, et al. Use of visual inspection with acetic acid, Pap smear, or high-risk human papillomavirus testing in women living with HIV/AIDS for posttreatment cervical cancer screening:, same tests, different priorities. Aids, 2017, 31(2):233. https://doi.org/10.1097/QAD.0000000000001327

[17] Rahman M F, Akhter S N, Alam M J, et al. Detection of Cervical Cancer through Visual Inspection of Cervix with Acetic Acid (VIA) and Colposcopy at Mymensingh Medical College Hospital. Mymensingh Medical Journal Mmj, 2016, 25(3):402.

[18] Chigbu C O, Onyebuchi A K, Nnakenyi E F, et al. Impact of visual inspection with acetic acid plus cryotherapy "see and treat" approach on the reduction of the population burden of cervical preinvasive lesions in Southeast Nigeria. Nigerian Journal of Clinical Practice, 2017, 20(2):239. https://doi.org/10.4103/1119-3077.187315

[19] Panagiotis Ntovas, Nikolaos Loubrinis, Panagiotis Maniatakos. Evaluation of dental explorer and visual inspection for the detection of residual caries among Greek dentists. Journal of Conservative Dentistry Jcd, 2018, 21(3):311. https://doi.org/10.4103/JCD.JCD_67_17

[20] Gatot Purwoto, Hasra Depiesa Dianika, Andre Putra. Modified Cervicography and Visual Inspection with Acetic Acid as an Alternative Screening Method for Cervical Precancerous Lesions. Journal of Cancer Prevention, 2017, 22(4):254-259. https://doi.org/10.15430/JCP.2017.22.4.254

[21] Sondang Sidabutar, Santi Martini, Chatarina Umbul Wahyuni. Analysis of Factors Affecting Women of Childbearing Age to Screen Using Visual Inspection with Acetic Acid. Osong Public Health & Research Perspectives, 2017, 8(1):61. https://doi.org/10.24171/j.phrp.2017.8.1.08

[22] Wallace Mukupa, Craig Hancock, Gethin Roberts. Visual inspection of fire-damaged concrete based on terrestrial laser scanner data. Applied Geomatics, 2017, 9(12):1-16. https://doi.org/10.1007/s12518-017-0188-9

[23] Licia Aguilar Freitas, Maria Teresa Botti Rodrigues Santos, Renata Oliveira Guare. Association between Visual Inspection, Caries Activity Status, and Radiography with Treatment Decisions on Approximal Caries in Primary Molars. Pediatric Dentistry, 2016, 38(2):140-147.

[24] Oliver Chukwujekwu Ezechi, Karen Odberg Petterson, Titilola A Gbajabiamila. Evaluation of Direct Visual Inspection of the Cervix in Detecting Cytology Diagnosed Squamous Intraepithelial Lesion in Women of known HIV Status. A Randomized Trial (CANHIV Study). African Journal of Reproductive Health, 2016, 20(4):77-88. https://doi.org/10.29063/ajrh2016/v20i4.8

[25] Xiaochun Lu, Juntao Fei. Velocity Tracking Control of Wheeled Mobile Robots by Iterative Learning Control. International Journal of Advanced Robotic Systems, 2016, 13(3):1. https://doi.org/10.5772/63813

[26] Seokwon Yeom, Yong-Hyun Woo. Person-Specific Face Detection in a Scene with Optimum Composite Filtering and Colour-Shape Information. International Journal of Advanced Robotic Systems, 2013, 10(1):1. https://doi.org/10.5772/54239

[27] Tianjiang Hu, Shuyuan Wang, Han Zhou. Theoretical Insights on Contraction-Type Iterative Learning Control for Biorobotic Systems with Preisach Hysteresis. International Journal of Advanced Robotic Systems, 2016, 13(3):1. https://doi.org/10.5772/63632

[28] Padulo J, Pizzolato F, Rodrigues S T, et al. Task complexity reveals expertise of table tennis

players. J Sports Med Phys Fitness, 2016, 56(1-2):149-156.

[29] Zhang, Kun, Cao, Zhiqiang, Liu, Jianran. Real-Time Visual Measurement With Opponent Hitting Behavior for Table Tennis Robot. IEEE Transactions on Instrumentation & Measurement, 2018, 67(4):811-820. https://doi.org/10.1109/TIM.2017.2789139

[30] Su, Hu, Xu, De, Chen, Guodong, Fang, Zaojun, Tan, Min, & Hu Su. A learning model for racket motion decision in ping-pong robotic system. Asian Journal of Control, 2016, 18(1):236-246. https://doi.org/10.1002/asjc.1009

[31] Marcus Valtonen Örnhag, Heyden A. Generalization of Parameter Recovery in Binocular Vision for a Planar Scene. International Journal of Pattern Recognition & Artificial Intelligence, 2019, 33(11):563-578. https://doi.org/10.1142/S0218001419400111

[32] Schmid K L, Beavis S D, Wallace S I, et al. The Effect of Vertically Yoked Prisms on Binocular Vision and Accommodation. Optometry & Vision Science, 2019, 96(6):1. https://doi.org/10.1097/OPX.0000000000001388

[33] Li C, Zhou C, Miao C, et al. Binocular vision profilometry for large-sized rough optical elements using binarized band-limited pseudo-random patterns. Optics Express, 2019, 27(8):10890. https://doi.org/10.1364/OE.27.010890

[34] Congzheng W, Song H U, Chang F, et al. Deformation detection system of fuel assembly based on underwater binocular vision. Journal of Applied Optics, 2019, 40(2):58-63. https://doi.org/10.5768/JAO201940.0202001

[35] Jiang G, Luo M, Bai K. Optical positioning technology of an assisted puncture robot based on binocular vision. International Journal of Imaging Systems & Technology, 2019, 29(2):180-190. https://doi.org/10.1002/ima.22303